Default Mode Network Functional Connectivity in Early and Late Mild Cognitive Impairment

Results From the Alzheimer's Disease Neuroimaging Initiative

Eek-Sung Lee, MD,† Kwangsun Yoo, PhD,† Young-Beom Lee, MS,† Jinyong Chung, BSc,† Ji-Eun Lim,† Bora Yoon, MD, PhD,‡ and Yong Jeong, MD, PhD,*† for the Alzheimer's Disease Neuroimaging Initiative*

Background: Default mode network (DMN) functional connectivity is one of the neuroimaging candidate biomarkers of Alzheimer disease. However, no studies have investigated DMN connectivity at different stages of mild cognitive impairment (MCI). The aim of this study was to investigate patterns of DMN connectivity and its breakdown among cognitively normal (CN), early MCI (EMCI), and late MCI (LMCI) subjects.

Methods: Magnetic resonance imaging data and neuropsychological test scores from 130 subjects (CN = 43, EMCI = 47, LMCI = 40) were obtained from the Alzheimer's Disease Neuroimaging Initiative. DMN functional connectivity was extracted using independent components analysis and compared between groups.

Results: Functional connectivity in the precuneus, bilateral medial frontal, parahippocampal, middle temporal, right superior temporal, and left angular gyri was decreased in EMCI subjects compared with CN subjects. When the 2 MCI groups were directly compared, LMCI subjects exhibited decreased functional connectivity in the precuneus, bilateral medial frontal gyri, and left angular gyrus. There was no significant difference in gray matter volume among the 3 groups. Amyloid-positive EMCI subjects revealed more widespread breakdown of DMN connectivity than amyloid-negative EMCI subjects. A quantitative index of DMN connectivity correlated well with measures of cognitive performance.

Conclusions: Our results suggest that the breakdown of DMN connectivity may occur in the early stage of MCI.

Key Words: Alzheimer disease, mild cognitive impairment, default mode network, functional connectivity, resting-state fMRI

(*Alzheimer Dis Assoc Disord* 2016;30:289–296)

Received for publication February 16, 2015; accepted December 28, 2015.

From the *Graduate School of Medical Science and Engineering; †Laboratory for Cognitive Neuroscience and NeuroImaging, Department of Bio and Brain Engineering, Korea Advanced Institute of Science and Technology; and ‡Department of Neurology, Konyang University Hospital, College of Medicine, Konyang University, Daejeon, Republic of Korea.

E.-S.L. and K.Y. contributed equally.

Data used in preparing this article were obtained from the Alzheimer's Disease Neuroimaging Initiative (ADNI) database (http://www.loni.ucla.edu/ADNI). As such, investigators within the ADNI contributed to the design and implementation of the ADNI and/or provided data but did not participate in the analysis or writing of this report. For a complete listing of ADNI investigators, please see: http://adni.loni.ucla.edu/wp-content/uploads/how_to_apply/ADNI_Manuscript_Citations.pdf.

Author contributions: E.S.L. and K.Y.: conception design, data analysis and interpretation, and manuscript writing. Y.B.L., J.C., and J.E.L.: data analysis and interpretation. Y.J. and B.Y.: final approval of manuscript, data analysis and interpretation, and manuscript writing.

The authors declare no conflicts of interest.

Reprints: Yong Jeong, MD, PhD, Department of Bio and Brain Engineering, Korea Advanced Institute of Science and Technology (KAIST), 291 Daehak-ro, Yuseong-gu, Daejeon 305-701, Republic of Korea (e-mail: yong@kaist.ac.kr) and Bora Yoon, MD, PhD, Department of Neurology, Konyang University Hospital, College of Medicine, Konyang University, Daejeon, Republic of Korea (e-mail: boradori3@hanmail.net).

Supplemental Digital Content is available for this article. Direct URL citations appear in the printed text and are provided in the HTML and PDF versions of this article on the journal's Website, www.alzheimerjournal.com.

Pathologic changes involved in Alzheimer disease (AD) begin many years before the clinical expression of dementia.[1] Recent advances in neuroimaging and cerebrospinal fluid (CSF) biomarker screening allow the possibility of detecting AD during its early stages and have led to changes in its diagnostic criteria.[2,3] Thus, AD is now considered as a dynamic disease with a spectrum of cognitive states ranging from cognitively normal (CN) to mild cognitive impairment (MCI) to dementia. There is growing consensus that the target population for disease-modifying therapy is not individuals with dementia but rather those with MCI or preclinical AD.[4]

The Alzheimer's Disease Neuroimaging Initiative (ADNI) recently subdivided MCI into early (EMCI) and late (LMCI) MCI stages on the basis of the severity of impaired delayed recall of logical memory.[5,6] Several researchers have investigated the potential use of neuroimaging findings as biomarkers for EMCI and LMCI.[7–9] In a diffusion tensor imaging study of ADNI, there was no significant difference between CN and EMCI groups, whereas the LMCI group showed differences in mean diffusivity, radial diffusivity, and axial diffusivity in the left hippocampal part of the cingulum.[7] In another study, the LMCI group showed reduced overall cortical thickness compared with CN and EMCI groups, but there was no difference between CN and EMCI groups.[8] Furthermore, brain glucose metabolism remains normal in individuals with EMCI despite the presence of significant amyloid accumulation.[9] Therefore, despite an established concept of EMCI, significant EMCI-related brain abnormalities as revealed by neuroimaging are not well documented, except for amyloid deposition based on amyloid positron emission tomography (PET) using florbetapir.

These neuroimaging abnormalities (ie, cortical thinning, glucose hypometabolism, and amyloid deposition) in the MCI stage are mainly localized in the entorhinal and posterior medial cortical areas.[7–9] The posteromedial cortical areas are known to be functionally connected with entorhinal cortex[10–12] and to play a key role in memory function in MCI and dementia.[13,14] These regions are also core regions of default mode network (DMN).[15]

The DMN, which becomes less active during engagement in cognitive tasks and more active during rest, has received much attention as a potential AD biomarker.[16,17] Several neuroimaging studies show that DMN areas overlap with areas of amyloid plaque deposition,[18] and functional connectivity in the DMN is disrupted in both AD and MCI.[19–21] As functional connectivity in the DMN has been noted to have an impact on the episodic memory, breakdown of DMN connectivity could be an underlying reason behind the memory loss in AD.[22]

One notable study demonstrated that DMN connectivity indices can distinguish between individuals with MCI who will and will not convert to AD.[23] Main findings of that study were that an index of DMN connectivity for MCI nonconverters was higher than that for MCI converters, and baseline DMN connectivity indices were correlated with cognitive decline from the baseline. From these findings, it could be speculated that MCI subjects with more disrupted DMN connectivity are at greater risk to convert to AD.

Applying the same criteria for EMCI and LMCI proposed in ADNI, the annual conversion rate to AD in the EMCI subjects (12%) were much less than that observed in LMCI subjects (27%).[5] On the basis of the previous literature that DMN functional connectivity is predictive of conversion from MCI to AD,[23] we can hypothesize that DMN connectivity of LMCI subjects is more disrupted than EMCI subjects. However, there has been no study focusing on DMN abnormalities at different stages of MCI, such as EMCI and LMCI.

In the present study, we used resting functional magnetic resonance imaging (fMRI) to investigate the breakdown of DMN functional connectivity across the continuum from CN to EMCI to LMCI using a well-established data-driven method. We examined whether this breakdown in functional connectivity corresponds with cognitive decline during the MCI stage.

MATERIALS AND METHODS

Subjects and Data Acquisition

Data were obtained from the ADNI database (adni.loni.usc.edu). The primary goal of ADNI is to test whether the results of serial MRI, PET, biological assays, and clinical and neuropsychological assessments can be combined to assess the progression of MCI and early AD.

From the ADNI database, we obtained data for all available 124 participants (45 CN, 49 EMCI, and 40 LMCI) who completed the following clinical, imaging, and neuropsychological assessments during a single visit: Mini Mental State Examination (MMSE), Montreal Cognitive Assessment (MoCA), Functional Activities Questionnaire (FAQ), clinical dementia rating-sum of box score (CDR-SOB), ADNI composite score for memory and executive function (ADNI-Mem and ADNI-EF),[24,25] apolipoprotein E epsilon 4 carrier status, and resting-state fMRI. Of these 124 participants, 4 were excluded because of poor image quality (eg, excessive head motion, severe artifacts, or partial brain coverage). The remaining 120 subjects (43 CN, 47 EMCI, and 40 LMCI) were included in further analyses. Florbetapir mean standard uptake value ratio data were downloaded from the ADNI public database (ida.loni.use.edu). The florbetapir positivity cutoff value was set at 1.11.[26] Detailed diagnostic, inclusion, and exclusion criteria are described on the ADNI website (http://www.adni-info.org).

Preprocessing and Independent Component Analysis (ICA) of Resting-state fMRI Data

Preprocessing of fMRI data and ICA were carried out as described previously.[27] All steps were performed using Statistical Parametric Mapping 8 (SPM8, http://www.fil.ion.ucl.ac.uk/spm/software/spm8/) and Group ICA of fMRI Toolbox (GIFT, v1.3i, http://mialab.mrn.org/software) in MATLAB R2011a (Natick, MA). The first 2 fMRI volumes were discarded for signal stabilization before preprocessing. A slice timing correction was performed for the fMRI time series, and spatially realigned fMRI time series images were coregistered with T1 MRI. T1 data were used as a normalization source image to register the fMRI images into the Montreal Neurological Institute (MNI)-152 template. Transformation matrices from individual T1s to the MNI template were calculated, and these matrices were applied to each coregistered fMRI image. Finally, normalized fMRI images were smoothed using an isotropic Gaussian kernel of 6 mm full-width at half maximum to increase the signal to noise ratio. We extracted 20 group-independent components. The reason for extracting 20 components was based on a previous report, which compared ICA methods, components, and resting-state networks. This study showed the overall highest consistency of temporal and spatial correlations when 20 components was used as a parameter.[28] DMN components were identified by selecting components with the highest spatial correlation to the DMN template supplied by GIFT software. Visual inspections assured that the selected components resembled the DMN. No false selection of the template-based automated procedure was observed. Individual DMN components extracted from group ICA were converted into z-score maps.

Preprocessing of Structural T1 Data and Voxel-based Morphometry (VBM) Analysis

VBM using T1 images was performed to investigate possible contributions that gray matter (GM) loss may have on DMN breakdown. Preprocessing of structural T1 data was performed using DARTEL (Diffeomorphic Anamoical Registration Through Exponentiated Lie algebra) implemented in SPM8.[29] Firstly, structural T1 images were segmented into the GM, the white matter, and the cerebrospinal fluid using the tissue priority maps, and GM maps were spatially normalized. Then, spatially normalized GM maps were modulated to adjust volume changes during nonlinear transformation. Finally, normalized GM maps were smoothed using the Gaussian kernel of 8 mm full-width at half maximum, and smoothed images were used for VBM. Regional GM volume was compared using 1-way analysis of variance in SPM8. Statistical significance was set at $P < 0.05$, family-wise error (FWE) corrected, with a cluster extent threshold of 50.

TABLE 1. Demographics of 130 Subjects

	CN (n = 43)	EMCI (n = 47)	LMCI (n = 40)	*P*	Post Hoc
Age (SD) (y)	74.5 (5.8)	71.4 (6.8)	71.4 (8.1)	0.053	
Female, n (%)	25 (58.1)	28 (59.6)	16 (40.0)	0.136	
Education (SD) (y)	16.1 (2.2)	15.5 (2.5)	16.9 (2.5)	0.028	EMCI < LMCI
APOE ϵ4 carriers, n (%)	14 (32.6)	24 (51.1)	17 (42.5)	0.114	
MMSE (SD)	28.7 (1.4)	28.0 (1.8)	27.7 (1.6)	0.010	CN > LMCI
MoCA (SD)	25.4 (2.0)	24.1 (2.8)	22.4 (3.2)	< 0.001	CN = EMCI > LMCI
FAQ (SD)	0.3 (1.1)	2.7 (4.0)	4.5 (5.3)	< 0.001	CN < EMCI = LMCI
CDR-SOB (SD)	0.1 (0.5)	1.4 (1.0)	1.8 (1.1)	< 0.001	CN < EMCI = LMCI
ADNI-Mem (SD)	0.84 (0.42)	0.44 (0.49)	0.10 (0.39)	< 0.001	CN > EMCI > LMCI
ADNI-EF (SD)	0.78 (0.64)	0.47 (0.73)	0.23 (0.86)	0.004	CN > LMCI
Florbetapir + , n (%)*	13 (33.3)	28 (60.9)	24 (60.0)	0.019	CN < EMCI = LMCI
GM volume (SD) (mL)	596.9 (60.86)	588.3 (60.7)	592.7 (58.38)	0.797	

*Missing data: 4 CN, 1 EMCI.

ADNI-EF indicates composite score for executive function; ADNI-Mem, composite score for memory; APOE, apolipoprotein E; CDR-SOB, clinical dementia rating-sum of box score; CN, cognitively normal; EMCI, early mild cognitive impairment; FAQ, functional activities questionnaire; GM, gray matter; ICV, intracranial volume; LMCI, late cognitive impairment; MMSE, Mini Mental State Examination; MoCA, Montreal Cognitive Assessment.

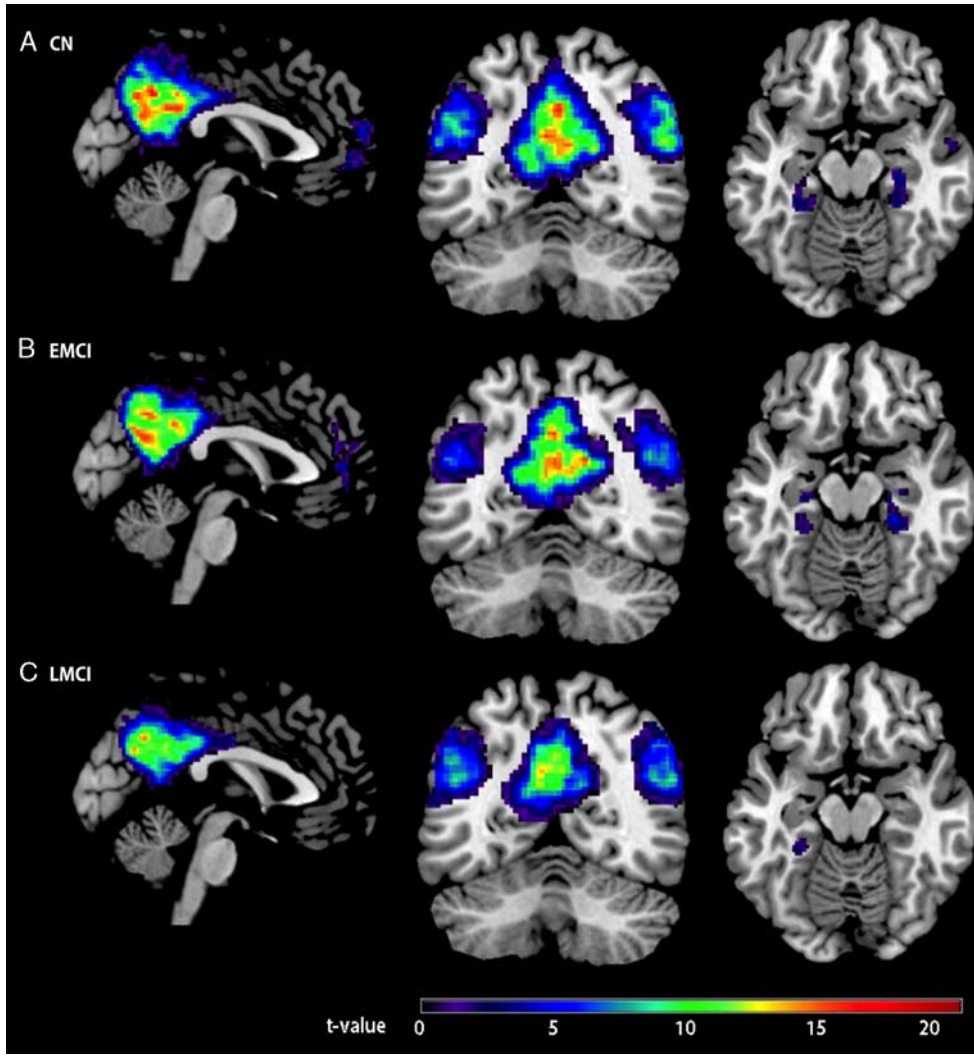

FIGURE 1. Average DMN connectivity maps for CN, EMCI, and LMCI subjects. In the DMN of CN (A) and EMCI (B) subjects, significant clusters include the posterior cingulate/precuneus, bilateral inferior parietal lobules, and parahippocampal gyri. Note that there is no significant cluster in the right parahippocampal gyrus in LMCI subjects (C). The cover overlays the results of 1-sample *t* tests corrected for multiple comparisons using a family-wise error correction ($P < 0.05$). CN indicates cognitively normal; DMN, default mode network; EMCI, early mild cognitive impairment; LMCI, late mild cognitive impairment.

Calculation of Mean DMN z-score

To calculate individual mean DMN z-scores, a DMN mask was first created using a 1-sample t test of individual DMN components in the CN group, thresholded by a FWE-corrected $P < 0.05$ and a cluster extent of 15. The mean z-score of all voxels within the DMN mask was calculated using MATLAB.[16,30]

Statistical Analysis

Statistical analysis was performed using the Statistical Package for the Social Sciences (SPSS) for Windows v18.0 (SPSS Institute Inc., Chicago, IL). Significance levels for all analyses were set at $P < 0.05$. Group comparisons of clinical and imaging variables were assessed using analysis of variance with Tukey post hoc analysis for parametric continuous variables, Kruskal-Wallis tests for nonparametric continuous variables, and χ^2 tests for categorical variables. Individual DMN components from each group were introduced into a voxel-wise group statistical analysis with age, sex, education, and GM volume as covariates using SPM8. Group analysis included testing the significance of average connectivity maps for each group (1-sample t test) and group differences (1-way analysis of variance). To investigate the possible confounding effects of amyloid burden in the DMN connectivity, EMCI subjects were classified as amyloid-positive EMCI ($A\beta^+$ EMCI) and amyloid-negative EMCI ($A\beta^-$ EMCI) according to florbetapir mean standard uptake value ratio. Statistical significance was set at $P < 0.05$, FWE-corrected, with a cluster extent threshold of 15. Partial correlations,

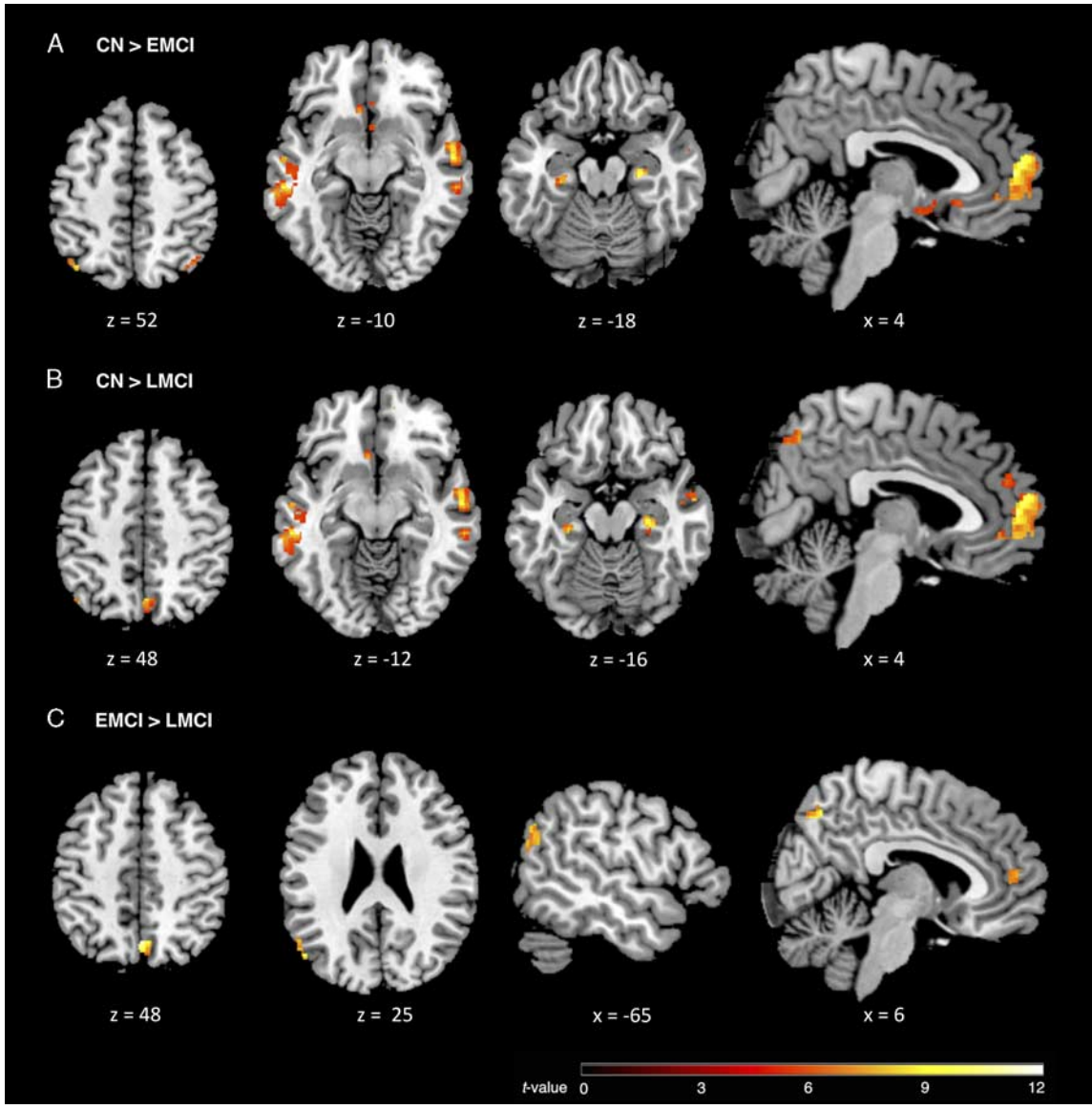

FIGURE 2. Group difference DMN connectivity maps for CN, EMCI, and LMCI subjects. Decreased DMN connectivity in EMCI subjects compared with CN subjects (A), in LMCI subjects compared with CN subjects (B), and in LMCI subjects compared with EMCI subjects (C). All difference maps are thresholded at a family-wise error–corrected $P < 0.05$ with a cluster threshold >15. Inverse contrasts (CN < EMCI, CN < LMCI, and EMCI < LMCI) do not show significant differences among groups. CN indicates cognitively normal; DMN, default mode network; EMCI, early mild cognitive impairment; LMCI, late mild cognitive impairment.

controlling for age, sex, and education, were used to assess the relationship between DMN *z*-score and clinical variables such as MMSE, MoCA, FAQ, CDR-SOB, ADNI-Mem, and ADNI-EF scores. Bonferroni correction was applied for multiple comparisons.

RESULTS

Demographic and neuropsychological characteristics of CN, EMCI, and LMCI subjects are shown in Table 1. As expected, LMCI subjects showed poorer performance than CN subjects in all neuropsychological tests. EMCI and LMCI subjects did not differ on the scores of MMSE, ADNI-EF, CDR-SOB, and FAQ. ADNI-Mem scores were significantly different among the 3 groups. CN and EMCI subjects differed on CDR-SOB and FAQ. Age, sex, and APOE $\epsilon 4$ carrier status of all groups did not differ significantly, but LMCI subjects had more years of education than EMCI subjects. There was no significant difference in GM volume between the 3 groups, but the percentage of florbetapir-positive subjects was significantly higher in the EMCI and LMCI groups than in the CN group.

Results of average DMN maps for the CN, EMCI, and LMCI groups are illustrated in Figure 1. CN and EMCI subjects showed significant clusters in the precuneus, posterior cingulate cortex, medial prefrontal cortex, bilateral lateral parietal cortex, and bilateral medial temporal lobe (Figs. 1A, B). LMCI subjects showed significant clusters only in the precuneus, posterior cingulate cortex, left and right lateral parietal cortex, and left medial temporal lobe (Fig. 1C).

Figure 2 and Table 2 show the results of voxel-wise group comparisons of DMN functional connectivity. EMCI and LCMI subjects showed decreased DMN functional connectivity in the precuneus, bilateral medial frontal, parahippocampal, middle temporal gyri, right superior temporal gyrus, and left angular gyrus compared with CN subjects. In addition, LMCI subjects exhibited decreased functional connectivity in the right superior frontal and left superior temporal gyrus compared with CN subjects (Figs. 2A, B). Furthermore, LMCI subjects exhibited decreased functional connectivity in the precuneus, bilateral medial frontal gyri, and left angular gyrus compared with EMCI subjects (Fig. 2C). In the subgroup analysis, $A\beta^+$ EMCI subjects revealed more widespread decreased connectivity in the DMN than $A\beta^-$ EMCI subjects compared with CN subjects (Supplement Table 1, Supplemental Digital content 1, http://links.lww.com/WAD/A135). In the VBM analysis, there was no significant difference of GM volume between the 3 groups.

Considering all 3 groups, mean DMN *z*-score, a quantitative measure of DMN connectivity, was positively correlated with MoCA ($r = 0.326$, $P < 0.05$, Bonferroni corrected), ADNI-Mem ($r = 0.369$, $P < 0.05$, Bonferroni corrected), and ADNI-EF ($r = 0.319$, $P < 0.05$, Bonferroni corrected) scores and negatively correlated with CDR-SOB ($r = -0.270$, $P < 0.05$, Bonferroni corrected) (Fig. 3). There was no significant correlation between DMN *z*-score and MMSE and FAQ. When we performed this analysis in each of the groups (CN, EMCI, or LMCI), no statistically significant results were obtained.

DISCUSSION

The main finding of our study is that EMCI involves significant breakdown of functional connectivity in key DMN regions, including the precuneus, bilateral medial frontal, parahippocampal, middle temporal, right superior temporal gyri, and left angular gyrus. These are the main regions responsible for amyloid deposition and the disruption of DMN connectivity in AD.[18–20,30,31] To the best of our knowledge, this is the first examination of functional connectivity in the DMN at different stages of MCI.

TABLE 2. Brain Clusters Showing Significant Differences Among Groups

Contrast	Brain Region	Cluster Size (Voxels)	Peak MNI Coordinates (mm)		
			X	*Y*	*Z*
CN > EMCI	Precuneus	11	2	−68	56
	Bilateral medial frontal gyrus	658	2	60	16
	Right parahippocampal gyrus	56	28	−20	−18
	Right middle temporal gyrus	322	58	−4	−14
	Right superior temporal gyrus	18	60	−56	22
	Left Parahippocampal gyrus	42	−28	−28	−16
	Left middle temporal gyrus	208	−58	−32	−10
	Left angular gyrus	22	−40	−70	50
CN > LMCI	Precuneus	57	0	−66	50
	Bilateral medial frontal gyrus	688	2	60	16
	Right superior frontal gyrus	17	22	34	58
	Right parahippocampal gyrus	60	28	−20	−18
	Right middle temporal gyrus	331	58	−4	−14
	Right superior temporal gyrus	37	42	16	−30
	Left parahippocampal gyrus	44	−28	−28	−16
	Left middle temporal gyrus	99	−58	−32	−10
	Left superior temporal gyrus	47	−54	−62	24
	Left angular gyrus	46	−54	−64	28
EMCI > LMCI	Precuneus	56	0	−66	50
	Bilateral medial frontal gyrus	39	6	52	10
	Left angular gyrus	64	−42	−72	42

CN indicates cognitively normal; EMCI, early mild cognitive impairment; LMCI, late mild cognitive impairment.

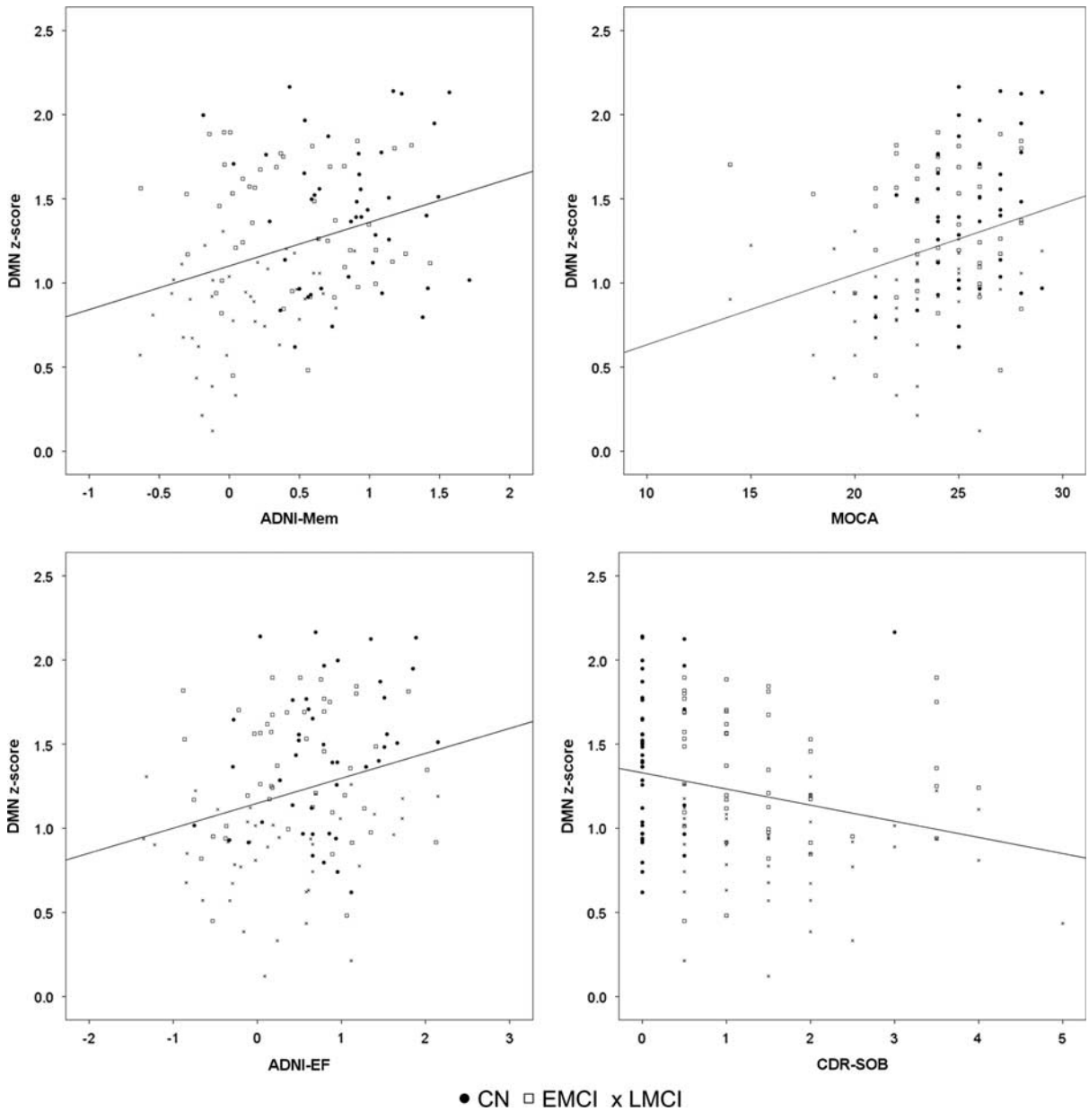

FIGURE 3. Correlations between mean DMN *z*-score and neuropsychological test scores. Black dots represent CN, black squares EMCI, and black crosses LMCI. Mean DMN *z*-score is positively correlated with MoCA ($r=0.326$, $P<0.05$, Bonferroni corrected), ADNI-Mem ($r=0.369$, $P<0.05$, Bonferroni corrected), and ADNI-EF ($r=0.319$, $P<0.05$, Bonferroni corrected) scores and negatively correlated with CDR-SOB ($r=-0.270$, $P<0.05$, Bonferroni corrected). ADNI-EF indicates composite score for executive function; ADNI-Mem, composite score for memory; CDR-SOB, clinical dementia rating-sum of box score; CN, cognitively normal; DMN, default mode network; EMCI, early mild cognitive impairment; LMCI, late mild cognitive impairment; MoCA, Montreal Cognitive Assessment.

DMN connectivity is a well-replicated neuroimaging finding of AD.[16,17,20,21,23] We found that EMCI subjects showed decreased DMN functional connectivity, which is consistent with other studies showing decreased functional connectivity of the DMN in elderly CN individuals with high amyloid burden,[31,32] individuals with presenilin-1 mutations,[33] and carriers of apolipoprotein E epsilon 4 (APOE ϵ4).[34,35] We also investigated whether GM atrophy contributed to DMN connectivity. There was no significant difference of GM volume among 3 groups in the VBM analysis. Group difference of DMN connectivity remained significant after adjusting for the GM volume as a covariate, suggesting that DMN connectivity differences were independent of GM atrophy. Taken together, the present and previous studies indicate that disruption of DMN connectivity might be one of the earliest neuroimaging abnormalities of AD.

Although not all individuals with EMCI convert to dementia, our results indicate that this group represents an early symptomatic stage of AD. Moreover, LMCI subjects showed additional disruption of DMN connectivity, suggesting that LMCI closely resembles AD in terms of DMN

functional connectivity. Our findings suggest that DMN functional connectivity might deteriorate progressively from CN to EMCI to LMCI stages. Furthermore, DMN functional connectivity was positively correlated with clinical measures of cognitive ability, such as MoCA, ADNI-Mem, and ADNI-EF scores, and negatively correlated with CDR-SOB scores. These findings are also consistent with those of earlier studies.[16,36,37]

Outcomes of recent clinical trials on disease-modifying therapies for AD have been disappointing. As a result, there is growing consensus that the optimal population for clinical trials is not demented individuals but rather predemented individuals on the spectrum of AD neurobiology.[4,5] For this reason, the concept of EMCI has been gaining attention as the earliest symptomatic stage of AD.[7–9,26] A previous study shows that brain metabolism remains normal despite the presence of significant amyloid accumulation in EMCI, suggesting that the EMCI stage is an optimal period for antiamyloid intervention.[9] In this regard, our results suggest the value of neuroimaging findings for diagnosis and intervention during the EMCI stage.

Several points should be carefully considered when interpreting our results. The percentage of amyloid-positive subjects based on amyloid PET using florbetapir in the EMCI group (60.9%) was higher than that in a previous study,[38] which might contribute to the observed breakdown of DMN functional connectivity in EMCI subjects. This variability between studies could be due to different sampled populations. Because our study focused on resting functional connectivity, we included subjects only if they underwent resting-state fMRI, which may have resulted in differences in sampled populations even though both studies used the same ADNI data set. $A\beta^+$ EMCI subjects showed more widespread breakdown of DMN connectivity than $A\beta^-$ EMCI subjects in our subgroup analysis; it might be speculated that amyloid burden affects breakdown of DMN connectivity in EMCI subjects. Another consideration is that our study utilized a cross-sectional design. Thus, we were unable to observe longitudinal changes in DMN connectivity during AD progression within individuals or unable to determine the proportion of individuals with EMCI who progress to LMCI and then to AD. Lastly, we could not assess levels of CSF tau and $A\beta_{42}$, which could possibly be related to changes in DMN connectivity. Thus, future longitudinal studies that examine CSF biomarkers are needed to address these issues.

ACKNOWLEDGMENTS

This research was supported by a grant of the Korea Health Technology R&D Project through the Korea Health Industry Development Institute (KHIDI), funded by the Ministry of Health & Welfare, Republic of Korea (grant number: HI14C2768).

Data collection and sharing for this project was funded by the ADNI (National Institutes of Health Grant U01 AG024904) and Department of Defense (DoD) ADNI (Award number W81XWH-12-2-0012). ADNI is funded by the National Institute on Aging, the National Institute of Biomedical Imaging and Bioengineering, and through generous contributions from the following sponsors: Alzheimer's Association; Alzheimer's Drug Discovery Foundation; BioClinica Inc.; Biogen Idec Inc.; Bristol-Myers Squibb Company; Eisai Inc.; Elan Pharmaceuticals Inc.; Eli Lilly and Company; F. Hoffmann-La Roche Ltd and its affiliated company Genentech Inc.; GE Healthcare; Innogenetics, N.V.; IXICO Ltd.; Janssen Alzheimer Immunotherapy Research & Development, LLC.; Johnson & Johnson Pharmaceutical Research & Development LLC.; Medpace Inc.; Merck & Co. Inc.; Meso Scale Diagnostics, LLC.; NeuroRx Research; Novartis Pharmaceuticals Corporation; Pfizer Inc.; Piramal Imaging; Servier; Synarc Inc.; and Takeda Pharmaceutical Company. The Canadian Institutes of Health Research provides funds to support ADNI clinical sites in Canada. Private sector contributions are facilitated by the Foundation for the National Institutes of Health (http://www.fnih.org). The grantee organization is the Northern California Institute for Research and Education, and the study is coordinated by the Alzheimer's Disease Cooperative Study at the University of California, San Diego. ADNI data are disseminated by the Laboratory for Neuro Imaging at the University of Southern California. The funders had no role in study design, data collection and analysis, decision to publish, or preparation of the manuscript.

REFERENCES

1. Shim YS, Morris JC. Biomarkers predicting Alzheimer's disease in cognitively normal aging. *J Clin Neurol*. 2011;7:60–68.
2. Albert MS, DeKosky ST, Dickson D, et al. The diagnosis of mild cognitive impairment due to Alzheimer's disease: recommendations from the National Institute on Aging-Alzheimer's Association workgroups on diagnostic guidelines for Alzheimer's disease. *Alzheimers Dement*. 2011;7:270–279.
3. McKhann GM, Knopman DS, Chertkow H, et al. The diagnosis of dementia due to Alzheimer's disease: recommendations from the National Institute on Aging-Alzheimer's Association workgroups on diagnostic guidelines for Alzheimer's disease. *Alzheimers Dement*. 2011;7:263–269.
4. Sperling RA, Aisen PS, Beckett LA, et al. Toward defining the preclinical stages of Alzheimer's disease: recommendations from the National Institute on Aging-Alzheimer's Association workgroups on diagnostic guidelines for Alzheimer's disease. *Alzheimers Dement*. 2011;7:280–292.
5. Aisen PS, Petersen RC, Donohue MC, et al. Clinical Core of the Alzheimer's Disease Neuroimaging Initiative: progress and plans. *Alzheimers Dement*. 2010;6:239–246.
6. Weiner MW, Aisen PS, Jack CR Jr, et al. The Alzheimer's disease neuroimaging initiative: progress report and future plans. *Alzheimers Dement*. 2010;6:202–211.e207.
7. Nir TM, Jahanshad N, Villalon-Reina JE, et al. Effectiveness of regional DTI measures in distinguishing Alzheimer's disease, MCI, and normal aging. *Neuroimage Clin*. 2013;3:180–195.
8. Ye BS, Seo SW, Yang JJ, et al. Comparison of cortical thickness in patients with early-stage versus late-stage amnestic mild cognitive impairment. *Eur J Neurol*. 2014;21:86–92.
9. Wu L, Rowley J, Mohades S, et al. Dissociation between brain amyloid deposition and metabolism in early mild cognitive impairment. *PLoS One*. 2012;7:e47905.
10. Vogt BA, Vogt L, Laureys S. Cytology and functionally correlated circuits of human posterior cingulate areas. *Neuroimage*. 2006;29:452–466.
11. Cavanna AE, Trimble MR. The precuneus: a review of its functional anatomy and behavioural correlates. *Brain*. 2006;129(pt 3):564–583.
12. Lee JE, Park HJ, Song SK, et al. Neuroanatomic basis of amnestic MCI differs in patients with and without Parkinson disease. *Neurology*. 2010;75:2009–2016.
13. Whitwell JL, Petersen RC, Negash S, et al. Patterns of atrophy differ among specific subtypes of mild cognitive impairment. *Arch Neurol*. 2007;64:1130–1138.

14. Jicha GA, Parisi JE, Dickson DW, et al. Neuropathologic outcome of mild cognitive impairment following progression to clinical dementia. *Arch Neurol*. 2006;63:674–681.
15. Lim JS, Kang DW. Stroke connectome and its implications for cognitive and behavioral sequela of stroke. *J Stroke*. 2015;17: 256–267.
16. Balthazar MLF, de Campos BM, Franco AR, et al. Whole cortical and default mode network mean functional connectivity as potential biomarkers for mild Alzheimer's disease. *Psychiatry Res*. 2014;221:37–42.
17. Koch W, Teipel S, Mueller S, et al. Diagnostic power of default mode network resting state fMRI in the detection of Alzheimer's disease. *Neurobiol Aging*. 2012;33:466–478.
18. Klunk WE, Engler H, Nordberg A, et al. Imaging brain amyloid in Alzheimer's disease with Pittsburgh Compound-B. *Ann Neurol*. 2004;55:306–319.
19. Bai F, Watson DR, Yu H, et al. Abnormal resting-state functional connectivity of posterior cingulate cortex in amnestic type mild cognitive impairment. *Brain Res*. 2009;1302:167–174.
20. Greicius MD, Srivastava G, Reiss AL, et al. Default-mode network activity distinguishes Alzheimer's disease from healthy aging: evidence from functional MRI. *Proc Natl Acad Sci USA*. 2004;101:4637–4642.
21. Rombouts SARB, Barkhof F, Goekoop R, et al. Altered resting state networks in mild cognitive impairment and mild Alzheimer's disease: An fMRI study. *Hum Brain Mapp*. 2005; 26:231–239.
22. Sohn WS, Yoo K, Na DL, et al. Progressive changes in hippocampal resting-state connectivity across cognitive impairment: a cross-sectional study from normal to Alzheimer disease. *Alzheimer Dis Assoc Disord*. 2014;28:239–246.
23. Petrella JR, Sheldon FC, Prince SE, et al. Default mode network connectivity in stable vs progressive mild cognitive impairment. *Neurology*. 2011;76:511–517.
24. Crane PK, Carle A, Gibbons LE, et al. Development and assessment of a composite score for memory in the Alzheimer's Disease Neuroimaging Initiative (ADNI). *Brain Imaging Behav*. 2012;6:502–516.
25. Gibbons LE, Carle AC, Mackin RS, et al. A composite score for executive functioning, validated in Alzheimer's Disease Neuroimaging Initiative (ADNI) participants with baseline mild cognitive impairment. *Brain Imaging Behav*. 2012;6: 517–527.
26. Lim JS, Park YH, Jang JW, et al. Alzheimer's Disease Neuroimaging I. Differential white matter connectivity in early mild cognitive impairment according to CSF biomarkers. *PLoS One*. 2014;9:e91400.
27. Yoo K, Sohn WS, Jeong Y. Tool-use practice induces changes in intrinsic functional connectivity of parietal areas. *Front Hum Neurosci*. 2013;7:49.
28. Schopf V, Windischberger C, Kasess CH, et al. Group ICA of resting-state data: a comparison. *MAGMA*. 2010;23:317–325.
29. Ashburner J. A fast diffeomorphic image registration algorithm. *Neuroimage*. 2007;38:95–113.
30. Wang Y, Risacher SL, West JD, et al. Altered default mode network connectivity in older adults with cognitive complaints and amnestic mild cognitive impairment. *J Alzheimers Dis*. 2013;35:751–760.
31. Hedden T, Van Dijk KR, Becker JA, et al. Disruption of functional connectivity in clinically normal older adults harboring amyloid burden. *J Neurosci*. 2009;29:12686–12694.
32. Sperling RA, LaViolette PS, O'Keefe K, et al. Amyloid deposition is associated with impaired default network function in older persons without dementia. *Neuron*. 2009;63: 178–188.
33. Sala-Llonch R, Fortea J, Bartres-Faz D, et al. Evolving brain functional abnormalities in PSEN1 mutation carriers: a resting and visual encoding fMRI study. *J Alzheimers Dis*. 2013;36:165–175.
34. Damoiseaux JS, Seeley WW, Zhou J, et al. Gender modulates the APOE epsilon4 effect in healthy older adults: convergent evidence from functional brain connectivity and spinal fluid tau levels. *J Neurosci*. 2012;32:8254–8262.
35. Machulda MM, Jones DT, Vemuri P, et al. Effect of APOE epsilon4 status on intrinsic network connectivity in cognitively normal elderly subjects. *Arch Neurol*. 2011;68:1131–1136.
36. Cha J, Jo HJ, Kim HJ, et al. Functional alteration patterns of default mode networks: comparisons of normal aging, amnestic mild cognitive impairment and Alzheimer's disease. *Eur J Neurosci*. 2013;37:1916–1924.
37. Zhu DC, Majumdar S, Korolev IO, et al. Alzheimer's disease and amnestic mild cognitive impairment weaken connections within the default-mode network: a multi-modal imaging study. *J Alzheimers Dis*. 2013;34:969–984.
38. Landau SM, Mintun MA, Joshi AD, et al. Amyloid deposition, hypometabolism, and longitudinal cognitive decline. *Ann Neurol*. 2012;72:578–586.

